PHYSICAL REVIEW C VOLUME 23, NUMBER 2 FEBRUARY 1981

Microscopic study of $^3He(\alpha,\gamma)^7Be$ electric-dipole capture reaction

Q. K. K. Liu
School of Physics, University of Minnesota, Minneapolis, Minnesota 55455
*and Hahn-Meitner-Institut für Kernforschung, Berlin, West Germany**

H. Kanada
Department of Physics, Niigata University, Niigata, Japan

Y. C. Tang
School of Physics, University of Minnesota, Minneapolis, Minnesota 55455
(Received 3 October 1980)

The electric-dipole radiative capture reaction of ^3He by α, leading to the ground and first excited states of ^7Be, is considered. The wave functions used are the result of a single-channel $^3He+\alpha$ resonating-group calculation which yields not only correct ^3He separation energies in both of these ^7Be bound states, but also a satisfactory description of the $^3He+\alpha$ scattering angular distributions in the low-energy region. As in our previous ^7Li charge-form-factor study, the present investigation is entirely microscopic and has the following important characteristics: (i) totally antisymmetric wave functions are used, (ii) the c.m. motion is correctly accounted for, (iii) bound-state and continuum wave functions are obtained in a unified manner, and (iv) the wave functions used have correct asymptotic behavior. With *no* adjustable parameters, it is found that quite reasonable agreement with experiment can be obtained. In particular, the behavior of the branching ratio is satisfactorily reproduced. The only discrepancy is that the calculated total capture cross section is about 20–30 % too large, which is very likely related to the fact that, for simplicity, only the dominant $^3He+\alpha$ cluster configuration has been included in the calculation.

[NUCLEAR REACTIONS $^3He(\alpha,\gamma)$, $E=0.1$–4.0 MeV; calculated capture cross section and branching ratio with resonating-group wave functions.]

I. INTRODUCTION

In a recent investigation,[1] hereafter referred to as KLT, we have computed the charge form factor of ^7Li with a seven-nucleon wave function obtained from a single-channel $t+\alpha$ resonating-group study.[2,3] The results obtained were quite satisfactory. With *no* adjustable parameters, it was found that one can obtain not only a good agreement between calculated and empirically determined values for the rms charge radius and spectroscopic quadrupole moment,[4] but also a reasonable overall description of the charge form-factor behavior in the q^2 region up to 7 fm^{-2}.[5,6] Encouraged by this success, we proceed now to examine another interesting electromagnetic process involving the seven-nucleon system, namely, the electric dipole ($E1$) radiative capture reaction of ^3He by α, leading to the ground and first excited states of ^7Be. It is our opinion that this is a timely and useful study, because a careful examination of this particular reaction at very low energies is important for a thorough understanding of the solar-neutrino problem,[7] which is receiving extensive theoretical and experimental attention at the present moment.

For the analyses of experimental $^3He+\alpha$ radiative capture data,[8-10] there currently exist only macroscopic studies which do not explicitly take into account the many-nucleon nature of the various nuclei involved. Thus, in the calculation of Tombrello and Parker,[11] the region of strong interaction is not directly considered, but is only crudely accounted for by the introduction of two adjustable boundary-value parameters. To improve this calculation, Kim and Nagatani[12] have recently performed another macroscopic calculation in which the interaction between the ^3He and α particles is represented by an effective, internuclear local potential. In view of the fact that the $^3He+\alpha$ effective interaction is known to be highly nonlocal in nature,[13] one must consider the calculation of these authors as overly simplified and, therefore, must examine their obtained results with considerable care.

In contrast, our calculation to be discussed below will be entirely microscopic and contains the following essential characteristics:

(i) Totally antisymmetric wave functions are used.

(ii) The center-of-mass motion is correctly treated.

(iii) Both bound-state and continuum wave functions are obtained in a unified manner.

(iv) The wave functions used have correct asymptotic behavior.

In addition, there will be *no* adjustable param-

eters. The bound-state and continuum wave functions adopted are the results of a single-channel ^{3}He + α resonating-group calculation, which yields not only correct ^{3}He separation energies in both the ground $\frac{3}{2}^-$ and the first excited $\frac{1}{2}^-$ states, but also a satisfactory description of the ^{3}He + α scattering results in the low-energy region.[2,3]

In the next section, we discuss the formulation of the capture problem and give a brief description of the ^{3}He + α resonating-group wave functions and results. Only the $E1$ contribution will be considered, since in the low-energy region the calculation of Tombrello and Parker[11] showed that other multipole contributions, such as $M1$ and $E2$, are not important. The results are presented in Sec. III, where comparisons will be made with both the older experimental values of Parker and Kavanagh[8] and Nagatani *et al.*,[9] and the more recent experimental values of the Münster group.[10] Finally, in Sec. IV we summarize the findings of this investigation and mention possible refinements which can be made to improve the present calculation.

II. FORMULATION

A. Resonating-group wave functions

The resonating-group formulation of the ^{3}He + α problem has been described elsewhere[2,3]; hence, only a brief recapitulation will be given here. Also, since we shall frequently refer to our recent $t + \alpha$ form factor calculation reported in KLT, we shall use, whenever possible, the same notation as that adopted in this particular reference.

In the single-channel approximation, the normalized final-channel bound-state ^{7}Be wave function, labeled by the total angular momentum J_f and its z component M_f, is written as

$$\psi_{J_f M_f} = C_{J_f} \mathcal{A} \bar{\psi}_{J_f M_f}, \tag{1}$$

where $\mathcal{A}$ is an antisymmetrization operator, C_{J_f} is a normalization factor, and

$$\bar{\psi}_{J_f M_f} = \phi_A \phi_B \left[\frac{1}{R} f_{J_f l_f}(R) \mathcal{Y}^{M_f}_{J_f l_f S} \right] Z(\vec{R}_{\text{c.m.}}). \tag{2}$$

Since we are concerned with the radiative capture not only to the ground $\frac{3}{2}^-$ state but also to the first excited $\frac{1}{2}^-$ state of ^{7}Be, we need J_f equal to either $\frac{3}{2}$ or $\frac{1}{2}$ with $l_f = 1$. In Eq. (2), the function $\mathcal{Y}^{M_f}_{J_f l_f S}$ is a spin-isospin-angle function, appropriate for $T = \frac{1}{2}$ and $S = \frac{1}{2}$. Its explicit form is

$$\mathcal{Y}^{M_f}_{J_f l_f S} = \sum_{\mu_f, M'_s} C(l_f S J_f; \mu_f M'_s M_f) Y^{\mu_f}_{l_f}(\hat{R}) \xi^{M'_s}_S, \tag{3}$$

with $C(l_f S J_f; \mu_f, M'_s, M_f)$ being a Clebsch-Gordan coefficient in the notation of Rose[14] and $\xi^{M'_s}_s$ being a spin-isospin function having M'_s for the z component of the spin angular momentum.

The functions ϕ_A and ϕ_B in Eq. (2) represent the internal spatial structures of the α and ^{3}He clusters, respectively. They are assumed to have the normalized forms

$$\phi_A = \left(\frac{\alpha_A^3}{4\pi^3} \right)^{3/4} \exp\left[-\tfrac{1}{2} \alpha_A \sum_{i=1}^{4} (\vec{r}_i - \vec{R}_A)^2 \right], \tag{4}$$

$$\phi_B = \left(\frac{\alpha_B^2}{3\pi^2} \right)^{3/4} \exp\left[-\tfrac{1}{2} \alpha_B \sum_{i=5}^{7} (\vec{r}_i - \vec{R}_B)^2 \right], \tag{5}$$

where $\vec{R}_A$ and $\vec{R}_B$ are, respectively, the c.m. coordinates of the two clusters. The width parameters are taken to be

$$\alpha_A = 0.514 \text{ fm}^{-2}, \tag{6}$$

$$\alpha_B = 0.367 \text{ fm}^{-2}, \tag{7}$$

which reproduce the rms matter radii deduced from electron-scattering experiments.[15] The function $Z(\vec{R}_{\text{c.m.}})$ describes the motion of the total center of mass. It is conveniently chosen as

$$Z(\vec{R}_{\text{c.m.}}) = \left(\frac{N_A \alpha_A + N_B \alpha_B}{\pi} \right)^{3/4} \times \exp[-\tfrac{1}{2}(N_A \alpha_A + N_B \alpha_B) \vec{R}_{\text{c.m.}}^{\,2}], \tag{8}$$

with $N_A = 4$ and $N_B = 3$ being the nucleon numbers of the α and ^{3}He clusters, respectively. This particular form is chosen, since we shall employ in this calculation the complex-generator-coordinate technique (CGCT)[16,17] which was specifically devised to facilitate computations of matrix elements in resonating-group studies where clusters with *unequal* width parameters are involved.

The relative-motion function $f_{J_f l_f}(R)$ is obtained as the solution of the projection equation

$$\langle \delta\psi_{J_f M_f} | H - E_T | \psi_{J_f M_f} \rangle = 0, \tag{9}$$

where E_T is the total energy of the system composed of cluster internal energies and the relative energy E of the two clusters in the c.m. system, and H is a Galilean-invariant Hamiltonian operator given by

$$H = \sum_{i=1}^{N} T_i + \sum_{i<j=1}^{N} V_{ij} - T_{\text{c.m.}}, \tag{10}$$

with

$$N = N_A + N_B \tag{11}$$

and $T_{\text{c.m.}}$ being the kinetic-energy operator of the

total center of mass. For the nucleon-nucleon potential, we utilize the one adopted in KLT, with the minor modification that the parameters u, V_λ, and $V_{\lambda\tau}$ are slightly changed in order to reproduce precisely the ^3He separation energies in the ground and first excited states of ^7Be.[4] Thus we use

$$u=0.984,$$
$$V_\lambda=-38\ \text{MeV}, \tag{12}$$
$$V_{\lambda\tau}=206\ \text{MeV},$$

in our present calculation.

The initial-state continuum function will be labeled by the channel spin $S(=\frac{1}{2})$ and its z component M_s. It has the form

$$\psi^{(+)}_{SM_s}=\frac{1}{\sqrt{N!}}\mathcal{A}\bar{\psi}^{(+)}_{SM_s}, \tag{13}$$

with

$$\bar{\psi}^{(+)}_{SM_s}=\phi_A\phi_B\left\{\frac{1}{R}\sum_{l_i J_i}\sum_{M_i}[4\pi(2l_i+1)]^{1/2}i^{l_i}\times f_{J_i l_i}(R)C(l_i S J_i;0M_s M_i)\mathcal{Y}^{M_i}_{J_i l_i S}\right\}\times Z(\vec{R}_{c.m.}). \tag{14}$$

The relative-motion function $f_{J_i l_i}(R)$ will be normalized such that there is an incident Coulomb-distorted plane wave of unit amplitude in the asymptotic region; that is, outside the region of nuclear interaction ($R>R_0$), it will be chosen as

$$f_{J_i l_i}(R)=\frac{1}{k}\exp[i(\sigma_{l_i}+\delta_{J_i l_i})]\times[F_{l_i}(\eta,kR)\cos\delta_{J_i l_i}+G_{l_i}(\eta,kR)\sin\delta_{J_i l_i}]\quad(R>R_0), \tag{15}$$

where η is the Sommerfeld parameter and k is the wave number of the asymptotic relative motion. Also, F_{l_i}, G_{l_i}, and σ_{l_i} represent, respectively, the regular Coulomb function, irregular Coulomb function, and Coulomb phase shift of the l_ith partial wave, and $\delta_{J_i l_i}$ (i.e., $\delta^+_{l_i}$ or $\delta^-_{l_i}$) is the nuclear phase shift in the (J_i, l_i) partial-wave channel. As has been explained previously,[2] this latter phase shift can be obtained straightforwardly from the solution of the resonating-group projection equation.

B. Brief description of resonating-group results

From the projection equation (9), one obtains the integrodifferential equation satisfied by the relative-motion function. By solving this latter equation subject to the condition that, outside the region of nuclear interaction, $f_{J_f l_f}$ should become proportional to the Whittaker function,[18] one finds the ^3He separation energy in the ground or the first excited state of ^7Be.

As was mentioned in the preceding subsection, the experimental ^3He separation energies of the two ^7Be bound states are precisely reproduced if one adopts the nucleon-nucleon potential described in KLT, with the parameters given by Eq. (12). In Fig. 1, we depict the magnitudes of the relative-motion function $f_{3/2,1}$ or f_G of the ground state and the relative-motion function $f_{1/2,1}$ or f_E of the first excited state as a function of $R=n_h(0.24\ \text{fm})$. From this figure, one sees that these two functions are very similar in the region of strong nuclear interaction, but differ substantially when the value of R becomes large.

At a continuum energy, one solves the integrodifferential equation to obtain the scattering wave function in each (J_i, l_i) state and the corresponding phase shift. In Fig. 1, we show the behavior of the relative-motion function $f_{1/2,0}$ or f_J at a c.m. energy of $E=0.1$ MeV. Here one sees that, because of the high Coulomb barrier, this function has a rather small magnitude in the spatial region where the two clusters strongly overlap.

Phase-shift values at selected energies are tabulated in Table I. Using these values, one can easily calculate the scattering differential cross section. The results (solid lines) at 1.41 and 2.06 MeV are given in Fig. 2, where Rutherford cross sections (dashed lines) and experimental

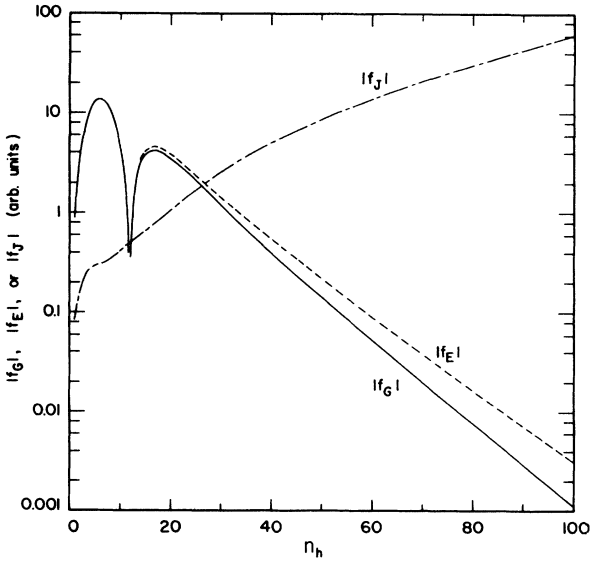

FIG. 1. Magnitudes of the relative-motion functions f_G of the ground state, f_E of the first excited state, and f_J (or $f_{1/2,0}$) of the continuum state at a c.m. energy of 0.1 MeV.

TABLE I. ^{3}He + α phase shifts (in degrees) as a function of E.

E (MeV)	δ_0	δ_1^+	δ_1^-	δ_2^+	δ_2^-	δ_3^+	δ_3^-
0.3	−0.15	−0.088	−0.12				
0.5	−1.10	−0.72	−0.94	−0.005	−0.005		
1.0	−6.93	−5.35	−6.53	−0.086	−0.090	0.036	0.031
1.41	−12.93	−10.82	−12.79	−0.26	−0.28	0.19	0.16
2.06	−21.88	−19.84	−22.79	−0.72	−0.78	1.13	0.86
2.65	−28.89	−27.48	−31.07	−1.20	−1.34	4.19	2.67
3.3	−35.52	−35.07	−39.18	−1.66	−1.93	20.52	7.71
4.0	−41.71	−42.39	−46.90	−1.91	−2.38	137.11	23.97

data[19] (solid dots) are also shown. From this figure, one notes that the agreement between calculation and experiment is generally satisfactory, being especially good in the forward angular region. This is important, because, for a reliable calculation of the ^{3}He + α radiative-capture cross section, one must at least demand that the scattering behavior be reasonably explained.

C. The $E1$ radiative-capture cross section

In the low-energy region which we are interested in, the long-wavelength limit (see the discussion given below in Sec. III C) of the $E1$ operator is a valid approximation. Thus, the cross section of $E1$ capture to a final state with total angular momentum J_f, accompanied by the emission of a γ ray of energy $E_\gamma = \hbar\omega$, is[20]

$$\sigma_{J_f}(E) = \frac{16\pi}{9}\frac{1}{\hbar v}\left(\frac{\omega}{c}\right)^3 B(E1), \tag{16}$$

where v is the relative velocity of the two nuclei at infinite separation, and $B(E1)$ is the reduced $E1$ transition probability having the form

$$B(E1) = \frac{e^2}{2S+1}\sum_{M_f M M_s} |\bar{Q}_{M_f M M_s}|^2, \tag{17}$$

with e being the proton charge. In the above equation, $\bar{Q}_{M_f M M_s}$, hereafter abbreviated as $\bar{Q}$, represents the transition matrix element and is given by

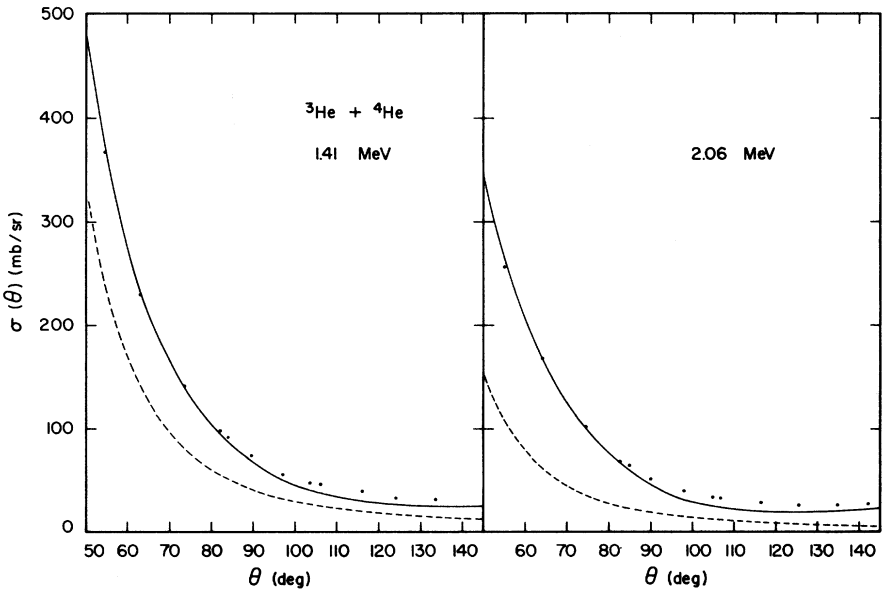

FIG. 2. Comparison of calculated (solid curve) and experimental (solid dots) ^{3}He + α differential cross sections at 1.41 and 2.06 MeV. The dashed curves represent the Rutherford cross sections at these energies.

$$\tilde{Q}=\left\langle\psi_{J_fM_f}\middle|\sum_{i=1}^{N}\mathfrak{M}^{E}_{1M}(i)\frac{1+\tau_{iz}}{2}\middle|\psi^{(+)}_{SM_s}\right\rangle$$

$$=\left\langle\psi_{J_fM_f}\middle|\sum_{i=1}^{N}\rho_i Y_1^{M*}(\hat{\rho}_i)\frac{1+\tau_{iz}}{2}\middle|\psi^{(+)}_{SM_s}\right\rangle, \quad (18)$$

where the nucleon spatial coordinate is measured relative to the coordinate of the total c.m., i.e.,

$$\vec{\rho}_i=\vec{r}_i-\vec{R}_{\text{c.m.}}\,. \quad (19)$$

For the evaluation of $\tilde{Q}$, it is convenient to write it as

$$\tilde{Q}=\frac{3}{4\pi i}\lim_{q\to 0}\frac{\partial}{\partial q}\int Y_1^{M*}(\hat{q})\left\langle\psi_{J_fM_f}\middle|\sum_{i=1}^{N}\exp[i\vec{q}\cdot(\vec{r}_i-\vec{R}_{\text{c.m.}})]\frac{1+\tau_{iz}}{2}\middle|\psi^{(+)}_{SM_s}\right\rangle d\hat{q}\,. \quad (20)$$

The matrix element appearing in the integrand on the right-hand side of Eq. (20) is the type which we considered in KLT. As was done there, the c.m. function is dealt with by using the fact that it appears in the wave functions [see Eqs. (1), (2), (13), and (14)] as a multiplicative factor; thus, we can write

$$\left\langle\psi_{J_fM_f}\middle|\sum_{i=1}^{N}\exp[i\vec{q}\cdot(\vec{r}_i-\vec{R}_{\text{c.m.}})]\frac{1+\tau_{iz}}{2}\middle|\psi^{(+)}_{SM_s}\right\rangle$$

$$=\left\langle\psi_{J_fM_f}\middle|\sum_{i=1}^{N}\exp(i\vec{q}\cdot\vec{r}_i)\frac{1+\tau_{iz}}{2}\middle|\psi^{(+)}_{SM_s}\right\rangle\frac{1}{F_{\text{c.m.}}}, \quad (21)$$

where

$$F_{\text{c.m.}}=\langle Z|\exp(i\vec{q}\cdot\vec{R}_{\text{c.m.}})|Z\rangle/\langle Z|Z\rangle$$

$$=\exp\left[-\frac{1}{4(N_A\alpha_A+N_B\alpha_B)}q^2\right]. \quad (22)$$

To evaluate the normalization factor C_{J_f} of this bound-state wave function, one uses the relation

$$|C_{J_f}|^2N!\langle\bar{\psi}_{J_fM_f}|\mathcal{A}\bar{\psi}_{J_fM_f}\rangle=1\,. \quad (23)$$

As has been mentioned in KLT, the computation of the factor $\langle\bar{\psi}_{J_fM_f}|\mathcal{A}\bar{\psi}_{J_fM_f}\rangle$ can be straightforwardly carried out. It is given by

$$\langle\bar{\psi}_{J_fM_f}|\mathcal{A}\bar{\psi}_{J_fM_f}\rangle=\sum_{\mu_f}[C(l_fSJ_f;\mu_f,M_f-\mu_f,M_f)]^2$$

$$\times\int G^*_{\mu_f}(\vec{R}')\mathfrak{N}(\vec{R}',\vec{R}'')$$

$$\times G_{\mu_f}(\vec{R}'')d\vec{R}'d\vec{R}'', \quad (24)$$

where

$$G_{\mu_f}(\vec{R}')=\frac{1}{R'}f_{J_fl_f}(R')Y^{\mu_f}_{l_f}(\hat{R}') \quad (25)$$

and

$$\mathfrak{N}(\vec{R}',\vec{R}'')=\mathfrak{N}_0(\vec{R}',\vec{R}'')+\sum_{x=1}^{N_B}\mathfrak{N}_x(\vec{R}',\vec{R}''), \quad (26)$$

with x ($1\le x\le N_B$, with $N_B<N_A$) being the number of nucleons interchanged between the α cluster (or cluster A) and the ^3He cluster (or cluster B). In Eq. (26), $\mathfrak{N}_0$ and $\mathfrak{N}_x$ represent the direct and exchange parts of the norm kernel; they have the forms

$$\mathfrak{N}_0(\vec{R}',\vec{R}'')=\delta(\vec{R}'-\vec{R}''), \quad (27)$$

$$\mathfrak{N}_x(\vec{R}',\vec{R}'')=(-1)^x\binom{N_B}{x}\frac{D_x}{D_0}\left(\frac{\pi^2}{a_xc_x}\right)^{3/2}$$

$$\times\exp[-A_x(\vec{R}'^2+\vec{R}''^2)-C_x\vec{R}'\cdot\vec{R}'']\,. \quad (28)$$

The constants A_x, C_x, D_x, D_0, a_x, and c_x are functions of N_A, α_A, N_B, α_B, and x. Their explicit expressions can be found in KLT.

The matrix element

$$\left\langle\psi_{J_fM_f}\middle|\sum_{i=1}^{N}\exp(i\vec{q}\cdot\vec{r}_i)\frac{1+\tau_{iz}}{2}\middle|\psi^{(+)}_{SM_s}\right\rangle$$

$$=C^*_{J_f}N!\left\langle\bar{\psi}_{J_fM_f}\middle|\sum_{i=1}^{N}\exp(i\vec{q}\cdot\vec{r}_i)\frac{1+\tau_{iz}}{2}\middle|\psi^{(+)}_{SM_s}\right\rangle \quad (29)$$

appearing in Eq. (21) can be evaluated in a parallel way as Eq. (43) of KLT. Thus, by combining Eqs. (18), (20), (21), and (29), one obtains

$$\tilde{Q}=C^*_{J_f}\sqrt{N!}\sum_{l_iJ_i}\sum_{\mu_i\mu_fM'_sM_i}C(l_iSJ_i;0M_sM_i)C(l_iSJ_i;\mu_iM'_sM_i)C(l_fSJ_f;\mu_fM'_sM_f)$$

$$\times C(l_fl_il;\mu_fM\mu_i)\left[\tilde{I}_0(J_il_i)+\sum_{x=1}^{N_B}\tilde{I}_x(J_il_i)\right]$$

$$=C^*_{J_f}\sqrt{N!}(-1)^{J_f-M-S}\sum_{l_iJ_i}[(2l_i+1)(2J_i+1)]^{1/2}C(l_iSJ_i;0M_sM_s)C(J_i1J_f;M_s,-M,M_f)$$

$$\times W(J_fl_fJ_il_i;S1)\left[\tilde{I}_0(J_il_i)+\sum_{x=1}^{N_B}\tilde{I}_x(J_il_i)\right], \quad (30)$$

where $W(J_f l_f J_i l_i; S1)$ is a Racah coefficient. The quantities $\bar{I}_0$ and $\bar{I}_x$ are the direct and exchange integrals; as in KLT, they can be further divided into different interaction types, i.e.,

$$\begin{aligned}
\bar{I}_0(J_i l_i) &= 2(\bar{I}_0^b + \bar{I}_0^c)\,, \\
\bar{I}_1(J_i l_i) &= 2(\bar{I}_1^{a1} + \bar{I}_1^{a2}) + 4(\bar{I}_1^b + \bar{I}_1^c)\,, \\
\bar{I}_2(J_i l_i) &= 4(\bar{I}_2^{a1} + \bar{I}_2^{a2}) + 2(\bar{I}_2^b + \bar{I}_2^c)\,, \\
\bar{I}_3(J_i l_i) &= 2(\bar{I}_3^{a1} + \bar{I}_3^{a2})\,,
\end{aligned} \tag{31}$$

where the superscript denotes the manner in which the single-particle $E1$ operator $\mathfrak{M}_{1M}^{E}(i)$ acts on a particular nucleon in the clusters. An explanation of the four types of interaction $a1$, $a2$, b, and c with the aid of the diagrammatical technique introduced by LeMere *et al.*[13] has been given in KLT. Below we give only the final expressions of these integrals:

(i) *Type a1.* The integral $\bar{I}_x^{a1}$ is given by

$$\begin{aligned}
\bar{I}_x^{a1}(J_i l_i) = T_x \sum_{l_\alpha l_\beta L} &(2l_\alpha+1)(2l_\beta+1)[3(2L+1)]^{1/2} i^{l_i} C(l_f l_\alpha L; 000) C(l_\alpha l_\beta 1; 000) C(L l_\beta l_i; 000) \\
&\times W(l_f l_\alpha l_i l_\beta; L1)\bar{\alpha}^{l_\alpha}\bar{\beta}^{l_\beta}\delta_{l_\alpha+l_\beta,1} P(J_i l_i; l_\alpha l_\beta L)\,,
\end{aligned} \tag{32}$$

with

$$T_x = (-1)^x \frac{D_x}{D_0}\left(\frac{\pi^2}{a_x c_x}\right)^{3/2}. \tag{33}$$

The quantity $P(J_i l_i; l_\alpha l_\beta L)$ is an integral of the form

$$\begin{aligned}
&P(J_i l_i; l_\alpha l_\beta L) \\
&= \int f_{J_f l_f}(R') R'^{l_\alpha} k_L(R', R'') R''^{l_\beta} f_{J_i l_i}(R'') dR' dR''\,,
\end{aligned} \tag{34}$$

where

$$\begin{aligned}
k_L(R', R'') = 4\pi(-1)^L R' R'' &\left(\frac{\pi}{2C_x R' R''}\right)^{1/2} \\
&\times I_{L+1/2}(C_x R' R'') \exp[-A_x(R'^2 + R''^2)]\,,
\end{aligned} \tag{35}$$

with A_x and C_x to be found in Eqs. (39) and (40) of KLT. The function $[\pi/(2C_x R' R'')]^{1/2} I_{L+1/2}(C_x R' R'')$ is a modified spherical Bessel function of the first kind.[18] Furthermore, the quantities $\bar{\alpha}$ and $\bar{\beta}$ can be written as

$$\bar{\alpha} = \omega'_{ax} + \lambda_{ax}\,, \tag{36}$$

$$\bar{\beta} = \omega''_{ax} + \lambda_{ax}\,, \tag{37}$$

in which ω'_{ax}, ω''_{ax}, and λ_{ax} are defined in Eqs. (49)–(55) of KLT.

(ii) *Type a2.* As was mentioned in KLT, this type is similar to type $a1$. The difference is that the roles of $\bar{\alpha}$ and $\bar{\beta}$ of Eqs. (36) and (37) are interchanged, i.e.,

$$\bar{\alpha} = \omega''_{ax} + \lambda_{ax}\,, \tag{38}$$

$$\bar{\beta} = \omega'_{ax} + \lambda_{ax}\,. \tag{39}$$

(iii) *Type b.* The integral $\bar{I}_0^b$ is given by

$$\begin{aligned}
\bar{I}_0^b = \gamma_b i^{l_i}[3(2l_f+1)]^{1/2} &C(l_f 1 l_i; 000) \\
&\times \int f_{J_f l_f}(R) R f_{J_i l_i}(R) dR\,,
\end{aligned} \tag{40}$$

with

$$\gamma_b = N_B/N\,. \tag{41}$$

The integral $\bar{I}_x^b$ has the same form as $\bar{I}_x^{a1}$, but with $\bar{\alpha}$ and $\bar{\beta}$ of Eqs. (36) and (37) to be replaced by

$$\bar{\alpha} = \bar{\beta} = \lambda_{bx}\,, \tag{42}$$

where λ_{bx} is defined in Eq. (62) of KLT.

(iv) *Type c.* The integrals $\bar{I}_0^c$ and $\bar{I}_x^c$ are very similar to the integrals $\bar{I}_0^b$ and $\bar{I}_x^b$. The integral $\bar{I}_0^c$ is the same as $\bar{I}_0^b$, except for the replacement of γ_b in Eq. (41) by

$$\gamma_c = -N_A/N\,. \tag{43}$$

Similarly, $\bar{I}_x^c$ is the same as $\bar{I}_x^b$, but with the $\bar{\alpha}$ and $\bar{\beta}$ of Eq. (42) to be replaced by

$$\bar{\alpha} = \bar{\beta} = \lambda_{cx}\,, \tag{44}$$

where λ_{cx} is defined in Eq. (68) of KLT.

Using Eq. (30), one can easily perform the summation in Eq. (17) over the magnetic quantum numbers M_f, M, and M_s, and obtain a final expression for the $E1$ radiative-capture cross section $\sigma_{J_f}(E)$. This expression is

$$\sigma_{J_f}(E)=\frac{16\pi}{9}\frac{e^2}{\hbar v}\left(\frac{\omega}{c}\right)^3\frac{1}{2S+1}|C_{J_f}|^2N! \times\sum_{J_i l_i}(2J_i+1)(2J_f+1)[W(J_f l_f J_i l_i;S1)]^2 \times\left|\bar{I}_0(J_i l_i)+\sum_{x=1}^{N_B}\bar{I}_x(J_i l_i)\right|^2, \quad (45)$$

in which one notes that the contributions from different (J_i, l_i) partial waves are summed incoherently. In the present case of $E1$ capture, the contributing partial waves have (J_i, l_i) equal to $(\frac{1}{2}, 0)$, $(\frac{3}{2}, 2)$, and $(\frac{5}{2}, 2)$.

At an incident c.m. energy E, one needs to consider capture processes leading to both the ground $\frac{3}{2}^-$ state and the first excited $\frac{1}{2}^-$ state. Thus, the total capture cross section is

$$\sigma_t(E)=\sigma_{3/2}(E)+\sigma_{1/2}(E). \quad (46)$$

In macroscopic studies of the capture process, nucleon-exchange effects are not explicitly taken into account. For example, if one omits the exchange terms in Eqs. (23) and (45), then the resultant expression for σ_{J_f} reduces to that derived by Christie and Duck.[21]

III. RESULTS AND DISCUSSIONS

A. Comparison with experimental results of Parker and Kavanagh, and Nagatani *et al.*

In Table II we show, at selected energies from 0.1 to 4 MeV, the calculated results for the capture cross section $\sigma_{3/2}$ to the ground state, the capture cross section $\sigma_{1/2}$ to the first excited state, the total capture cross section σ_t, and the branching ratio $\tilde{\rho}$ defined as

$$\tilde{\rho}=\sigma_{1/2}/\sigma_{3/2}. \quad (47)$$

TABLE II. Calculated results for capture cross sections and branching ratio.

E (MeV)	$\sigma_{3/2}$ (μb)	$\sigma_{1/2}$ (μb)	σ_t (μb)	$\tilde{\rho}$
0.10	0.000 326	0.000 136	0.000 462	0.417
0.15	0.004 32	0.001 80	0.006 12	0.417
0.20	0.019 0	0.007 91	0.026 9	0.417
0.30	0.100	0.041 8	0.142	0.417
0.40	0.251	0.105	0.356	0.418
0.50	0.448	0.188	0.636	0.420
0.75	1.02	0.433	1.45	0.424
1.00	1.58	0.676	2.26	0.429
1.41	2.41	1.05	3.46	0.437
1.70	2.96	1.30	4.26	0.440
2.06	3.63	1.61	5.24	0.443
2.65	4.69	2.09	6.78	0.444
3.30	5.84	2.60	8.44	0.445
4.00	7.08	3.14	10.22	0.443

From this table, one notes that even though the capture cross sections increase monotonically and rapidly with increasing energy, the branching ratio has a nearly constant value of around 0.43 over the whole energy range considered.

Calculated results for the total capture cross section are further depicted in Fig. 3, where for clarity an expanded version at very low energies is also given in the insert. In this figure, the data points shown are those of Parker and Kavanagh[8] (solid circles) and Nagatani *et al.*[9] (open circles). Here one sees that there is an overall satisfactory agreement between theory and experiment; in particular, the calculated cross section does increase with the same trend as the experimental result. However, the calculated values are somewhat too large. The reasons for this discrepancy are likely as follows.

(i) For the ground state of the mirror nucleus ^{7}Li, the rms charge radius obtained with a resonating-group wave function determined in a similar way as described here is equal to 2.44 fm (Ref. 1) which is about 2 to 3% larger than the empirical value.[5,6] A similar situation is expected to occur also in the ^{7}Be case. Since the radiative capture takes place mainly in the peripheral region, even this slight disagreement in the rms radius will result in a noticeable overestimate of the capture cross section.

(ii) The resonating-group wave function used in this investigation has a single $^3He+\alpha$ cluster configuration. For simplicity, other cluster configurations are not considered. Although it is anticipated that, at low energies, the $^3He+\alpha$ cluster structure should play a major role, the omission of other cluster structures will certainly affect the calculated result to a significant extent.

Both of these deficiencies mentioned above can be corrected by adding specific distortion effects into the present formulation. Within the resonating-group framework,[2] a proper consideration of such effects can be readily incorporated and has been made, for example, in the ^{6}Li system by many authors.[22-24]

In Fig. 4, a comparison is made between calculated and experimental values for the branching ratio $\tilde{\rho}$. Here again, the experimental data shown are those of Nagatani *et al.*[9] (open circles) and Parker and Kavanagh[8] (solid circles). As is seen, the property of near constancy is also exhibited

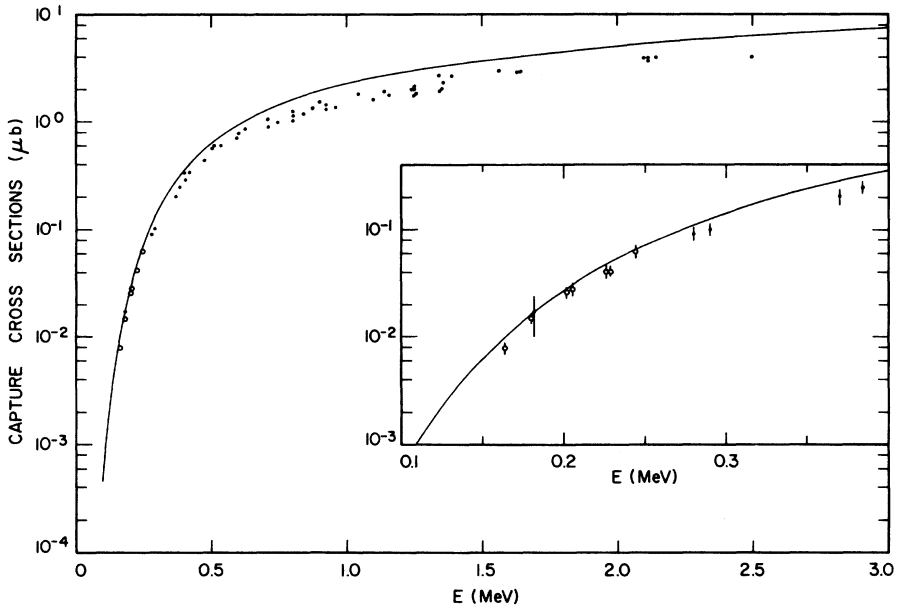

FIG. 3. Comparison of calculated and experimental total capture cross sections. The experimental data shown are those of Parker and Kavanagh (solid dots) and Nagatani *et al.* (open circles). The insert represents an expanded view of the comparison at very low energies.

by the experimental result. However, the calculated value of about 0.43 in the low-energy region of 0.2 to 1.4 MeV does seem to be somewhat higher than the measured values.

At very low energies, a more convenient way to compare calculated and experimental capture cross sections is through the so-called S factor $S(E)$, defined as[8]

$$S(E)=E\sigma_t(E)\exp(163.78/\sqrt{E}), \tag{48}$$

where E is expressed in units of keV. This is shown in Fig. 5. By using the calculated $S(E)$ values, one can make a reasonable extrapolation to yield a value of about 0.61 keV b for $S(0)$. This latter value is the same as that determined by Nagatani *et al.*[9] by a second-order polynomial fit of the empirical data, but is larger than the value of 0.47 ± 0.05 keV b quoted by Parker and Kavanagh.[8]

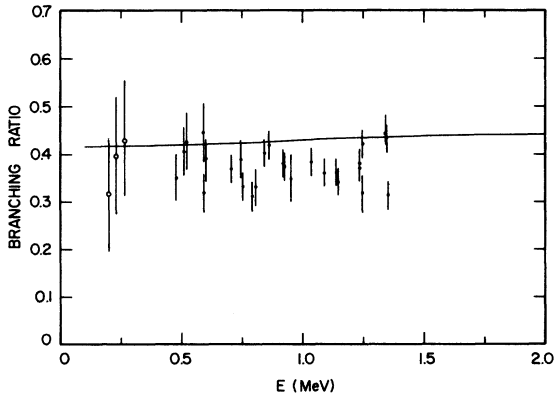

FIG. 4. Comparison of calculated and experimental branching ratios. The experimental data shown are those of Parker and Kavanagh (solid dots) and Nagatani *et al.* (open circles).

B. Comparison with experimental results of the Münster group

Recently, the $^3\mathrm{He}+\alpha$ radiative capture problem has been experimentally reconsidered by the Münster group.[10] In view of the fact that there is some substantial difference between their data, covering the energy range of 0.116 to 1.688 MeV, and the data of Parker and Kavanagh, and Nagatani

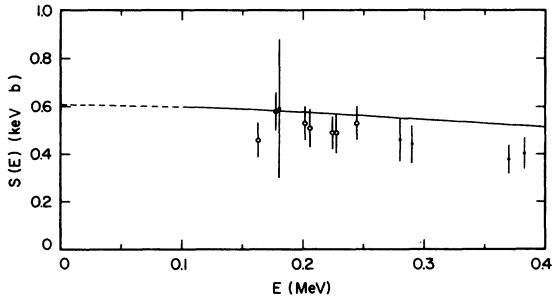

FIG. 5. Comparison of calculated and experimental S factors at very low energies. The empirical data shown are those of Parker and Kavanagh (solid dots) and Nagatani *et al.* (open circles). The dashed curve represents an extrapolation of the calculated values.

et al., we shall make in this subsection a separate comparison of our calculated values with the Münster result.

Calculated and experimental branching ratios are compared in the upper part of Fig. 6. Here one sees that the data points, which have generally uncertainties of about ± 0.03 (not shown in the figure, except for the typical point at 1.688 MeV and some points with particularly large uncertainties), lie on the average above the calculated curve. This is somewhat surprising, because our comparison with the results of Parker and Kavanagh, and Nagatani *et al.*, described in Sec. III A, showed just the opposite. However, one must note that both sets of experimental data exhibit rather large uncertainties and, hence, there may not be any serious inconsistency between them. On the other hand, it is clear that, for a better understanding of this important capture problem, there is the need of some data with higher accuracy.

The Münster group has so far not measured the absolute value of the capture cross section and, thus, only relative S factors at different energies were obtained. For a comparison with our calculation, what we do is, therefore, to normalize the experimental result to the theoretical value at 1.688 MeV. With this procedure, the resultant comparison is shown in the lower part of Fig. 6. As is seen, there is a rather satisfactory overall agreement; although it should be mentioned that, here again, more definitive conclusions can be drawn only when higher-quality, absolute cross-section measurements become available.

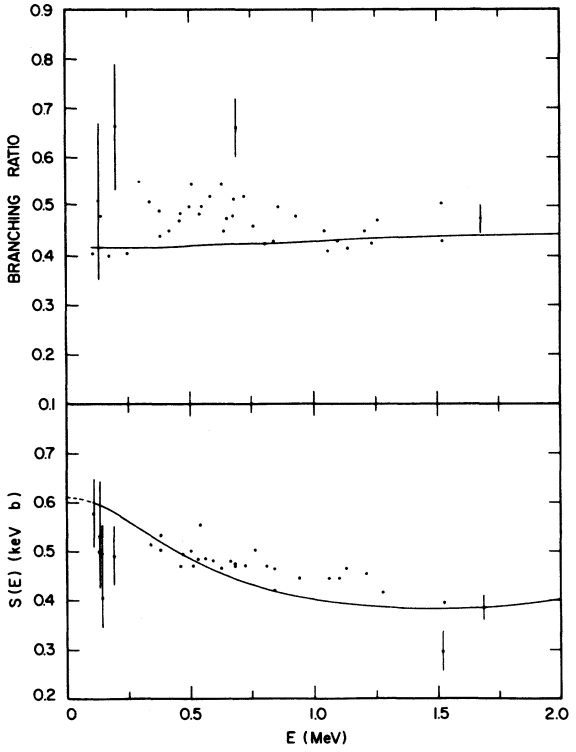

FIG. 6. Comparison of calculated and experimental branching ratios (upper part) and S factors (lower part). The experimental data (see text) are those of the Münster group (Ref. 10). For clarity, experimental errors bars are not shown, except for the typical point at 1.688 MeV and some points with particularly large uncertainties.

C. Contributions to the capture cross section

At very low energies, the radiative capture takes place mainly in the region outside of nuclear interaction but under the Coulomb barrier. To show this, we compute the quantities $\sigma_{3/2}(R_M)$ and $\sigma_{1/2}(R_M)$, obtained by setting the upper integration limits in Eqs. (34) and (40) as R_M instead of infinity. In Fig. 7, we depict at $E = 0.1$ MeV the behavior of the quantities $\eta_{3/2}$ [curve (a)] and $\eta_{1/2}$ [curve (b)], defined as

$$\eta_{3/2} = \sigma_{3/2}(R_M)/\sigma_{3/2}, \tag{49}$$

$$\eta_{1/2} = \sigma_{1/2}(R_M)/\sigma_{1/2}, \tag{50}$$

where $\sigma_{3/2}$ and $\sigma_{1/2}$ are given in Table II. From this figure, one finds that the values of R_M at the 10% and 90% points are, respectively, equal to 7.4 and 21.5 fm for the capture to the ground state, and 8.6 and 25.2 fm for the capture to the first excited state. In comparison, it should be noted that, at this energy, the classical turning distance has a large value of about 58 fm.

As the energy increases, the capture occurs more in the region where the nuclei are closer together. For the capture to the ground state, for

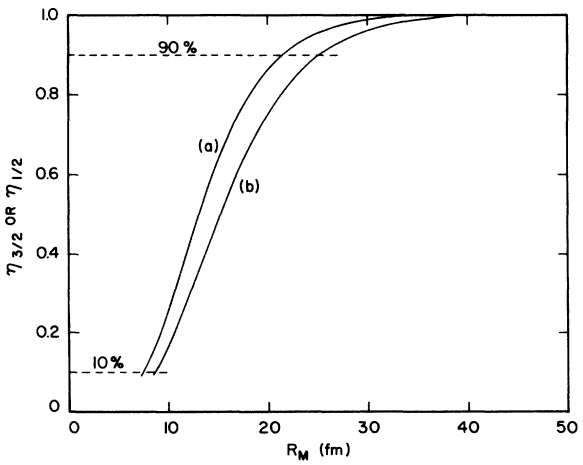

FIG. 7. Behavior of the quantities $\eta_{3/2}$ [curve (a)] and $\eta_{1/2}$ [curve (b)] at $E = 0.1$ MeV.

example, the R_M values of the 50% points at $E = 0.1$, 0.3, and 0.5 MeV are equal to 13.0, 11.9, and 10.9 fm, respectively, while the R_M values of the 90% points are equal to 21.5, 19.2, and 17.3 fm at these energies.

Even though at a very low energy the capture takes place predominantly at large separation distances, it is important to point out that the long-wavelength approximation for the $E1$ operator is still valid. This is indicated by the fact that the value of $\omega\bar{R}/c$, with $\bar{R}$ being the separation distance at which $\eta_{3/2}=0.5$, is still much smaller than 1. For instance, at $E=0.1$, 0.3, and 0.5 MeV, $\omega\bar{R}/c$ are equal to 0.111, 0.113, and 0.115, respectively.

Next, we consider the individual contributions $\sigma_{J_f}(J_i,l_i)$ [see Eq. (45)] from the incident (J_i,l_i) partial-wave channels. For this purpose, we define the quantities

$$\zeta_{J_i J_f} = \sigma_{J_f}(J_i l_i)/\sigma_{J_f}, \tag{51}$$

where σ_{J_f} at various energies are listed in Table II. The results for $\zeta_{J_i,3/2}$ and $\zeta_{J_i,1/2}$ are shown separately in Fig. 8, where the curves labeled (a), (b), and (c) refer to the cases with (J_i,l_i) equal to $(\frac{1}{2},0)$, $(\frac{5}{2},2)$, and $(\frac{3}{2},2)$, respectively. Here one sees that, as is expected, the contribution at very low energies comes mainly from the $l_i=0$ channel. On the other hand, it is clear by examining the behavior of these curves that the $l_i=2$ channels cannot be omitted from the calculation; already at $E=1.0$ MeV, the contribution from these channels amounts to more than 20%. A finding similar to this has also been reported by Tombrello and Parker.[11]

Another interesting feature is that, for the ground-state capture, the $l_i=2$ contribution comes predominantly from the $J_i=\frac{5}{2}$ state. For the capture to the first excited $J_f=\frac{1}{2}$ state, the $(\frac{5}{2},2)$ channel does not, of course, contribute to the $E1$ transition and, hence, only the $(\frac{3}{2},2)$ fractional contribution is shown.

IV. CONCLUSION

In this investigation, we have considered the electric-dipole radiative capture of $^3\mathrm{He}+\alpha$ to the ground and first excited states of $^7\mathrm{Be}$. The results show that, with *no* adjustable parameters, quite reasonable agreement with experiment can be obtained. In particular, the behavior of the branching ratio is satisfactorily reproduced. The only discrepancy is that the calculated total capture cross section is about 20–30% too large. As has been discussed, this is very likely related to the fact that, for simplicity, we have included only the dominant $^3\mathrm{He}+\alpha$ cluster configuration in the calculation.

The zero-energy S factor $S(0)$, obtained by an extrapolation of our calculated results at very low energies, is equal to 0.61 keV b. As in the case of the total capture cross section, this value is likely also 20–30% overestimated. To obtain a more realistic value, it will be necessary to carry

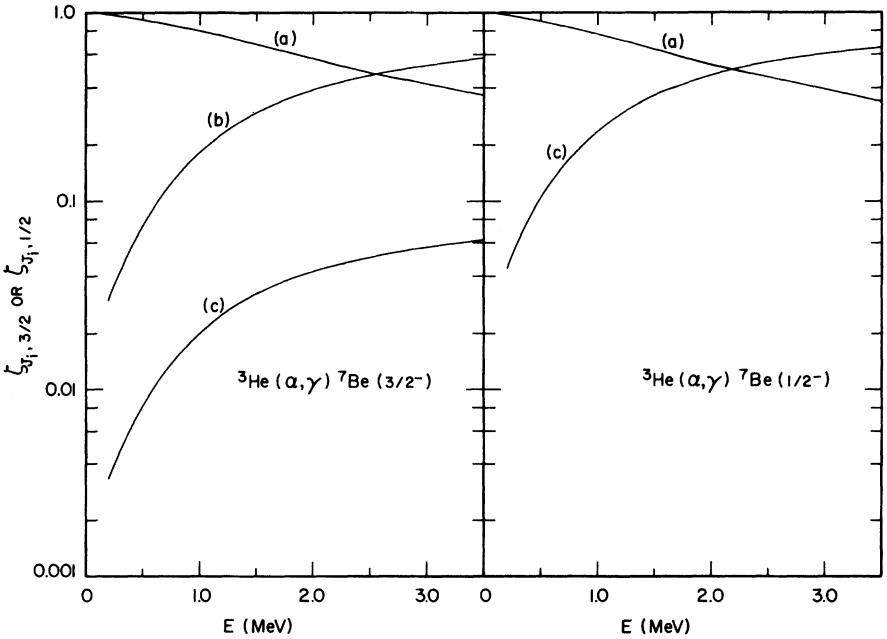

FIG. 8. Fractional contributions from various incident partial-wave channels. The curves labeled (a), (b), and (c) refer to the cases with $(J_i,l_i)=(\frac{1}{2},0)$, $(\frac{5}{2},2)$, and $(\frac{3}{2},2)$, respectively.

out a more refined calculation taking other cluster configurations also into account. This will be a rather tedious task but, in view of the important nature of this capture reaction in the solar-neutrino problem, is certainly worth performing.

The rather successful conclusions of both the present investigation and our previous study of the ^7Li charge form factor[1] indicate to us that the resonating-group wave functions used do yield a reasonable description of the essential behavior of the seven-nucleon system in the low-energy region. Therefore, one should proceed to examine other problems in this system, such as the electron capture of ^7Be,[4] the $M1$ and $M3$ form-factor study in ^7Li,[25] the $^3He+\alpha$ bremsstrahlung,[26,27] and so on. In addition, of course, it will be interesting to extend the present calculation to include other multipole transitions such that one can further study the angular distribution of the γ rays emitted in this capture reaction.

Note added. A recent article by Bahcall *et al.* [J. N. Bahcall, S. H. Lubow, W. F. Huebner, N. H. Magee, Jr., A. L. Merts, M. F. Argo, P. D. Parker, B. Rozsnyai, and R. K. Ulrich, Phys. Rev. Lett. 45, 945 (1980)] summarizes the present status of the solar-neutrino problem. In view of this, we wish to add some further, perhaps somewhat speculative, remarks based on our understanding and experience with the seven-nucleon system. Our extrapolated value of about 0.61 keV b for the zero-energy cross-section factor $S(0)$ is very likely an overestimate, the reason for this being clearly stated in Sec. III A. To obtain an improved value, one needs to first perform a more extensive resonating-group calculation, taking specific distortion effects properly into account. At present, we (together with T. Kaneko) have nearly completed such a calculation which should yield an even better description of the behavior of the seven-nucleon system in the low-energy region. Indeed, using the resultant bound-state wave function, we do find that the calculated values for the ^7Li charge form factor agree very well with empirical result at both low-q^2 and high-q^2 values. The $^3He+\alpha$ radiative-capture calculation, using this improved description, is planned for the immediate future. Prior to this latter calculation, we cannot, of course, state in any definitive manner about what the resultant value for $S(0)$ may turn out to be. However, considering the dominant nature of the $^3He+\alpha$ cluster configuration in the low-excitation region of ^7Be, we would venture to speculate that $S(0)$ will probably have a value around 0.45 keV b or somewhat higher. The low value of 0.34 keV b, a possibility discussed in the article of Bahcall *et al.*, is in our opinion not too likely.

ACKNOWLEDGEMENTS

One of us (Q.K.K.L.) wishes to thank Professor B. F. Bayman and Professor P. J. Ellis for the kind hospitality extended to him at the School of Physics, University of Minnesota. This research was supported in part by the U. S. Department of Energy under Contract No. DOE/DE-AC02-79 ER10364.

*Permanent address.

[1] H. Kanada, Q. K. K. Liu, and Y. C. Tang, Phys. Rev. C 22, 813 (1980).

[2] K. Wildermuth and Y. C. Tang, *A Unified Theory of the Nucleus* (Vieweg, Braunschweig, Germany, 1977).

[3] R. D. Furber, Ph.D. thesis, University of Minnesota, 1976 (unpublished).

[4] F. Ajzenberg-Selove, Nucl. Phys. A320, 1 (1979).

[5] L. R. Suelzle, M. R. Yearian, and H. Crannell, Phys. Rev. 162, 992 (1967).

[6] F. A. Bumiller, F. R. Buskirk, J. N. Dyer, and W. A. Monson, Phys. Rev. C 5, 391 (1972).

[7] C. A. Barnes, Adv. Nucl. Phys. 4, 133 (1971).

[8] P. D. Parker and R. W. Kavanagh, Phys. Rev. 131, 2578 (1963).

[9] K. Nagatani, M. R. Dwarakanath, and D. Ashery, Nucl. Phys. A128, 325 (1969).

[10] H. Krawinkel, K. U. Kettner, W. E. Kieser, C. Rolfs, R. Santo, P. Schmalbrock, H. P. Trautvetter, R. E. Azuma, and J. W. Hammer, Bereich Physiks Jahresbericht, Münster Universität, 1978-1979 (unpublished).

[11] T. A. Tombrello and P. D. Parker, Phys. Rev. 131, 2582 (1963).

[12] B. T. Kim and K. Nagatani, Bull. Am. Phys. Soc. 25, 594 (1980).

[13] M. LeMere, D. J. Stubeda, H. Horiuchi, and Y. C. Tang, Nucl. Phys. A320, 449 (1979).

[14] M. E. Rose, *Elementary Theory of Angular Momentum* (Wiley, New York, 1957).

[15] J. A. Koepke, R. E. Brown, Y. C. Tang, and D. R. Thompson, Phys. Rev. C 9, 823 (1974).

[16] Y. C. Tang, M. LeMere, and D. R. Thompson, Phys. Rep. 47, 167 (1978).

[17] D. R. Thompson and Y. C. Tang, Phys. Rev. C 12, 1432 (1975); 13, 2597 (1976).

[18] *Handbook of Mathematical Functions*, edited by M. Abramowitz and I. A. Stegun, National Bureau of Standards Applied Mathematics Series, No. 55 (U. S. G. P. O. Washington, D. C., 1972).

[19] A. C. L. Barnard, C. M. Jones, and G. C. Phillips, Nucl. Phys. 50, 629 (1964).

[20] S. A. Moszkowski, in *Alpha-, Beta-, and Gamma-Ray Spectroscopy*, edited by K. Siegbahn (North-Holland,

Amsterdam, 1966).
[21]R. F. Christie and I. Duck, Nucl. Phys. 24, 89 (1961).
[22]H. Jacobs, K. Wildermuth, and E. Wurster, Phys. Lett. 29B, 455 (1969).
[23]D. R. Thompson and Y. C. Tang, Phys. Rev. C 8, 1649 (1973).
[24]H. Kanada, T. Kaneko, H. Nishioka, and S. Saito, Prog. Theor. Phys. 63, 842 (1980).
[25]R. E. Rand, R. Frosch, and M. R. Yearian, Phys. Rev. 144, 859 (1966).
[26]H. Feshbach and D. R. Yennie, Nucl. Phys. 37, 150 (1962).
[27]B. Frois, J. Birchall, C. R. Lamontagne, U. von Muellendorff, R. Roy, and R. J. Slobodrian, Phys. Rev. C 8, 2132 (1973).